Prospects for observing dynamical and anti- dynamical Casimir effects in circuit QED due to fast modulation of qubit parameters

D S Veloso[1] and A V Dodonov[1,2]
[1] *Institute of Physics, University of Brasilia, 70910-900, Brasilia, Federal District, Brazil and*
[2] *International Center for Condensed Matter Physics, University of Brasilia, 70910-900, Brasilia, Federal District, Brazil*

We consider the nonstationary circuit QED architecture, where a single artificial two-level atom interacts with a cavity field mode under external modulation of one or more system parameters. Two different approaches are employed to study the effects of Markovian dissipation on modulation-induced transitions between the atom–field dressed states: the standard master equation of Quantum Optics and the recently formulated dressed-picture master equation. We estimate the associated transition rates and show that photon generation from vacuum ("dynamical Casimir effect", DCE) and coherent photon annihilation from nonvacuum states ("Anti-DCE") are possible with the current state-of-the-art parameters.

PACS numbers: 42.50.Pq, 42.50.Ct, 42.50.Hz, 32.80-t, 03.65.Yz

arXiv:1504.04783v1 [quant-ph] 19 Apr 2015

I. INTRODUCTION

The subject of photon generation in nonstationary circuit QED, where mesoscopic "artificial atoms" (constructed with Josephson junctions [1, 2]) interact with the Electromagnetic field confined in superconducting stripline resonators under nonstationary conditions [3], has been studied theoretically for nearly ten years. Traditionally one considered the externally prescribed modulation of either the cavity frequency [4–12], the atom–field coupling strength [13–17] or the atomic transition frequency [18–23], while recently more sophisticated schemes involving multi-level atoms, several qubits or coupled cavities were examined [10, 24–28]. Such a unique possibility of *in situ* control of the fundamental parameters of the Hamiltonian became possible thanks to the highly controllable solid state environment in which the system properties can be manipulated by external electric and magnetic fields [29–33]. Recently it was shown that modulation of *any* system parameter gives rise to similar effects of roughly the same order of magnitude, and simultaneous modulation of different parameters with the same frequency can increase or decrease the associated transition rate depending on the relative phases of modulations [34, 35]. Moreover, "multi-tone modulations" comprising two or more harmonic functions of time can lead to new types of effective interactions [21, 34, 35].

However, actual circuit QED architectures suffer from unavoidable dissipation effects, in particular, the damping of the cavity field, the atomic relaxation and the pure atomic dephasing [36]. Although some works on photon generation in nonstationary circuit QED analyzed the effects of losses [6, 13, 14, 25, 37], the majority of studies investigated only the unitary dynamics for different regimes of parameters and modulation shapes. Now that the general analytical description in absence of losses has been formulated in a closed form (under a series of approximations) [34, 35], the question of utmost practical interest is how dissipation affects the modulation-induced phenomena and whether they can be implemented with present or near-future technology.

So the goal of this work is to unveil which nonstationary phenomena can be implemented experimentally with the current technology [38–40] and comprehend how different dissipation channels affect the time evolution. We concentrate on the single-qubit, single-mode circuit QED setup and take into account the three aforementioned dissipation mechanisms using the Markovian and zero-temperature approximations. The master equation appropriate to this case, which takes into account the qubit–resonator coupling, was deduced microscopically in [36]. In this so called "dressed-picture master equation" (DPME) the dissipation rates depend on the spectrum of noise evaluated at the frequency matching the transition between the atom–field eigenstates (dressed states), so a prior knowledge of the bath structure is required. Besides, the analytical solution is complicated in majority of cases, so we carry out exact numerical simulations by assuming that the noise has a flat spectrum at positive frequencies and is zero for the negative ones. The details of the underlying mathematical formalism can be found in section II.

We consider several regimes of photon generation and annihilation due to modulation of the atomic transition frequency and the atom–field coupling strength. First we study the generation of two excitations from vacuum in the resonant regime (section III A) and the creation of one photon and one atomic excitation in the dispersive regime (*Anti-Jaynes-Cummings* behavior, section III B) for single-tone modulations. Then we analyze the recently discovered *Anti-dynamical Casimir effect* (Anti-DCE, section III C), whereby two excitations are coherently annihilated due to the modulation of qubit parameters in the dispersive regime [35]. We show that the above phenomena can be enhanced by using two-tone modulations (section IV), for which a total of four excitations can be generated from vacuum or annihilated from a known initial state. Quantum states with even

more excitations can be generated from vacuum in the dispersive regime via the *dynamical Casimir effect* (DCE, section V), when the system parameters are modulated with frequency roughly equal to twice the cavity unperturbed frequency.

It is shown that all the above phenomena can be implemented with current technology in dissipative circuit QED, although DCE and Anti-DCE require state-of-the-art dissipation rates and precise tuning of the modulation frequency. Moreover, we demonstrate numerically that for time intervals of interest the predictions of DPME are almost indistinguishable from the ones obtained for the "standard master equation" (SME) of Quantum Optics [41, 42], which is much simpler to handle and whose approximate solution is deduced here in the long-time limit.

II. MATHEMATICAL FORMALISM

The atom–field interaction is described by the Rabi Hamiltonian [21, 22, 43] and for generality we take into account the parametric amplification term due to eventual time-modulation of the cavity parameters [44]. The total Hamiltonian reads (we set $\hbar = 1$)

$$\hat{H} = \omega\hat{n} + \Omega|e\rangle\langle e| + g(\hat{a}+\hat{a}^\dagger)(\hat{\sigma}_+ + \hat{\sigma}_-) + i\chi(\hat{a}^{\dagger 2} - \hat{a}^2)\,, \quad (1)$$

where $\hat{a}$ and $\hat{a}^\dagger$ are cavity annihilation and creation operators and $\hat{n} = \hat{a}^\dagger\hat{a}$ is the photon number operator; $\hat{\sigma}_+ = |e\rangle\langle g|$ and $\hat{\sigma}_- = |g\rangle\langle e|$ are the atomic ladder operators, where $|g\rangle$ ($|e\rangle$) denotes the atomic ground (excited) state. ω is the cavity frequency, Ω is the atomic transition frequency, g is the atom–field coupling strength and χ is the squeezing coefficient related to the parametric amplification process. The time-independent part of χ may appear due to the terms proportional to the square of the vector potential [42], while the time-dependent part is due to the time-modulation of the cavity frequency and in the simplest case of DCE reads $\chi = (4\omega)^{-1}d\omega/dt$.

In this work we follow the convention of papers [34, 35] and suppose that all the system parameters can be perturbed simultaneously by external modulations of the form $X = X_0 + \varepsilon_X \sum_j w_X^{(j)} \sin(\eta^{(j)}t + \phi_X^{(j)})$. Here $X = \{\omega, \Omega, g, \chi\}$, X_0 and $\varepsilon_X \geq 0$ are the corresponding bare values and modulation depths, and the sum runs over all the fast modulation frequencies $\eta^{(j)} > \omega_0$. We consider small modulation depths given by inequalities $\varepsilon_\omega, \varepsilon_\Omega, \varepsilon_g\sqrt{n_{\max}}, \varepsilon_\chi n_{\max} \ll \omega_0$, where $n_{\max}$ is the maximum number of excitations. The parameters $w_X^{(j)} \geq 0$ and $\varphi_X^{(j)}$ are the relative weights and phase constants corresponding to the modulation of parameter X at frequency $\eta^{(j)}$. To shorten the notation we introduce the complex modulation depth $\varepsilon_X^{(j)} \equiv \varepsilon_X w_X^{(j)} \exp(i\phi_X^{(j)})$ that incorporates both the weight and the phase for the modulation frequency $\eta^{(j)}$. In our numerical examples the phases $\phi_X^{(j)}$ will always be set to zero and $w_X^{(j)} = 1$ for single-tone modulations with frequency $\eta^{(j)}$. Whenever more than one parameter are modulated simultaneously we shall call the process "multi-modulation".

We assume weak atom–field coupling, $g_0\sqrt{n_{\max}} \ll \omega_0$, and $\chi_0 = 0$, so one can describe the dynamics in the basis of eigenstates of the bare Jaynes-Cummings Hamiltonian (JCH) $\hat{H}_{JC} = \omega_0\hat{n} + \Omega_0|e\rangle\langle e| + g_0(\hat{a}\hat{\sigma}_+ + \hat{a}^\dagger\hat{\sigma}_-)$ [41, 42]. These states, known as *dressed states*, read

$$|\varphi_{n,\mathcal{S}}\rangle = \mathrm{s}_{n,\mathcal{S}}|g,n\rangle + \mathrm{c}_{n,\mathcal{S}}|e,n-1\rangle\,,\ n \geq 0\,,\ \mathcal{S} = \pm\,, \quad (2)$$

where n is the total number of system excitations and the index $\mathcal{S}$ labels different eigenstates with same n. We define formally $|\varphi_{0,+}\rangle \equiv 0$ and introduce the notation $\mathrm{s}_{m,-} = \mathrm{c}_{m,+} = \cos\theta_m$, $\mathrm{s}_{m,+} = -\mathrm{c}_{m,-} = \sin\theta_m$, where $\theta_0 = 0$, $\theta_{n>0} = \arctan[(\Delta_- + \beta_n)/(2g_0\sqrt{n})]$ and $\beta_n = \sqrt{\Delta_-^2 + 4g_0^2 n}$. The eigenenergies are $\lambda_{0,-} = 0$ and $\lambda_{n,\mathcal{S}} = \omega_0 n - \Delta_-/2 + \mathcal{S}\beta_n/2$, where $\Delta_- = \omega_0 - \Omega_0$ is the bare detuning (we assume $|\Delta_-| \ll \omega_0$).

The approximate unitary dynamics for the Hamiltonian (1) was solved in [34, 35] for arbitrary small-depth modulations. In the interaction picture defined by the unitary transformation $\hat{U}_t = \exp(-it\hat{H}_{JC})$ the effective Hamiltonian reads

$$\tilde{H} = \sum_{m,\mathcal{S},\mathcal{T}} \sum_j \Xi_{m,\mathcal{T},\mathcal{S}}^{(j)} e^{-it(\lambda_{m+2,\mathcal{S}} - \lambda_{m,\mathcal{T}} - \eta^{(j)})} \times |\varphi_{m,\mathcal{T}}\rangle\langle\varphi_{m+2,\mathcal{S}}| + h.c.\,, \quad (3)$$

where $m \geq 0$, $\mathcal{S}, \mathcal{T} = \pm$ and the time-independent coefficients $\Xi_{m,\mathcal{T},\mathcal{S}}^{(j)}$ will be given throughout the paper (the interaction-picture density operator is $\tilde{\rho} = \hat{U}_t^\dagger\hat{\rho}\hat{U}_t$). By choosing $\eta_M = \lambda_{M+2,\mathcal{S}} - \lambda_{M,\mathcal{T}}$ one resonantly couples the dressed states $|\varphi_{M,\mathcal{T}}\rangle \leftrightarrow |\varphi_{M+2,\mathcal{S}}\rangle$. If in addition $|\lambda_{m+2,\mathcal{S}} - \lambda_{m,\mathcal{T}} - \eta_M| \gg |\Xi_{m,\mathcal{T},\mathcal{S}}^{(j)}|$ for other values of $\{m, \mathcal{S}, \mathcal{T}\}$, all other terms can be neglected under the Rotating Wave Approximation (RWA) [34, 35] and one obtains a simplified time-independent Hamiltonian. Actually, the eigenenergies $\lambda_{n,\mathcal{S}}$ must be corrected by the so called "intrinsic frequency shifts" of the order $\mathrm{O}(g_0^2/\omega_0, \varepsilon_X^2/\omega_0)$ with $X = \{\omega, \Omega, g, \chi\}$. These corrections do not alter significantly the mathematical formalism, so we neglect them in the analytical derivations below; however, they will be incorporated into our numerical simulations to achieve exact resonances.

In the presence of dissipation the dynamics must be described by the master equation for the density operator

$$d\hat{\rho}/dt = -i[\hat{H}, \hat{\rho}] + \hat{\mathcal{L}}\hat{\rho}, \quad (4)$$

where $\hat{\mathcal{L}}$ is the Liouvillian superoperator. We shall use two different Markovian kernels to estimate the effects of dissipation. The quantum optical "standard master equation" (SME) at zero temperature is [41]

$$\hat{\mathcal{L}}_{SME}\bullet = \kappa\mathcal{D}[\hat{a}]\bullet + \gamma\mathcal{D}[\hat{\sigma}_-]\bullet + \frac{\gamma_\phi}{2}\mathcal{D}[\hat{\sigma}_z]\bullet\,, \quad (5)$$

where $\mathcal{D}[\hat{O}]\hat{\rho} \equiv \frac{1}{2}(2\hat{O}\hat{\rho}\hat{O}^\dagger - \hat{O}^\dagger\hat{O}\hat{\rho} - \hat{\rho}\hat{O}^\dagger\hat{O})$ is the Lindbladian superoperator and $\hat{\sigma}_z = |e\rangle\langle e| - |g\rangle\langle g|$. The constant parameters κ, γ and γ_ϕ denote the cavity damping,

qubit relaxation and the qubit pure dephasing rates, respectively.

The second approach is the "dressed-picture master equation" (DPME) at zero temperature developed in [36]

$$\mathcal{L}_{dr}\bullet = \mathcal{D}\left[\sum_l \Phi^l|l\rangle\langle l|\right]\bullet + \sum_{l,k\neq l}\Gamma_\phi^{lk}\mathcal{D}\left[|l\rangle\langle k|\right]\bullet + \sum_{l,k>l}\left(\Gamma_\kappa^{lk}+\Gamma_\gamma^{lk}\right)\mathcal{D}\left[|l\rangle\langle k|\right]\bullet, \quad (6)$$

where we use the shorthand notation $|l\rangle$ to denote the JCH dressed states $|\varphi_{n,\mathcal{S}}\rangle$, l increasing with the energy $\lambda_{n,\mathcal{S}}$. The parameters of equation (6) are defined as $\Phi^l = [\gamma_\phi(0)/2]^{1/2}\sigma_z^{ll}$, $\Gamma_\phi^{lk} = \gamma_\phi(\Delta_{kl})|\sigma_z^{lk}|^2/2$, $\Gamma_\kappa^{lk} = \kappa(\Delta_{kl})|a^{lk}|^2$ and $\Gamma_\gamma^{lk} = \gamma(\Delta_{kl})|\sigma_x^{lk}|^2$. Here $\kappa(\nu)$, $\gamma(\nu)$ and $\gamma_\phi(\nu)$ are the dissipation rates corresponding to the resonator and qubit dampings and dephasing noise spectral densities at frequency ν; we also defined $\Delta_{kl} = \lambda_k - \lambda_l$, $\sigma_z^{lk} = \langle l|\hat{\sigma}_z|k\rangle$, $a^{lk} = \langle l|(\hat{a}+\hat{a}^\dagger)|k\rangle$ and $\sigma_x^{lk} = \langle l|(\hat{\sigma}_+ + \hat{\sigma}_-)|k\rangle$. We do not consider a specific model for the reservoirs and make the simplest assumption that for $\nu \geq 0$ the dissipation rates are constant and equal to the corresponding rates of SME, while for $\nu < 0$ they are zero.

We shall solve both master equations exactly via numerical integration of the differential equations for the density matrix elements. We assume the usual value $\omega_0/2\pi = 8\,\mathrm{GHz}$ for the cavity frequency, high but feasible value $g_0 = 5\times10^{-2}\omega_0$ for the qubit–field coupling strength (within the weak coupling regime), moderate range of detuning $|\Delta_-| \leq 8g_0$ and the state-of-the-art dissipation rates $\kappa \sim \gamma \sim \gamma_\phi \sim 5\times10^{-5}g_0$ [38–40]. We presume the tentative value $|\Upsilon| \sim 10^{-2}$ for the collective relative modulation depth [$\Upsilon \sim \sum_X \varepsilon_X^{(j)}/X_0$, see equations (16), (21), (27), (48) below], small enough to fulfill the range of validity of the Hamiltonian (3) yet sufficient to implement the phenomena of interest.

A. Simplifications for the standard master equation

The interaction-picture density operator obeys the master equation

$$\frac{d\tilde{\rho}}{dt} = -i[\tilde{H},\tilde{\rho}] + \kappa\mathcal{D}[\tilde{a}]\tilde{\rho} + \gamma\mathcal{D}[\tilde{\sigma}_-]\tilde{\rho} + \frac{\gamma_\phi}{2}\mathcal{D}[\tilde{\sigma}_z]\tilde{\rho}, \quad (7)$$

where $\tilde{O} \equiv \hat{U}_t^\dagger\hat{O}\hat{U}_t$. The natural basis to expand $\tilde{\rho}$ consists of the JCH dressed states

$$\tilde{\rho}(t) = \sum_{n,m=0}^{\infty}\sum_{\mathcal{S},\mathcal{T}=\pm}\tilde{\rho}_{n,m}^{\mathcal{S},\mathcal{T}}(t)|\varphi_{n,\mathcal{S}}\rangle\langle\varphi_{m,\mathcal{T}}|\,. \quad (8)$$

By substituting equation (8) into (7) one can obtain the differential equations for the density matrix elements $\tilde{\rho}_{n,m}^{\mathcal{S},\mathcal{T}}(t)$. For example, for the pure atomic dephasing we get [using $\tilde{\rho}_{n,m}^{-,+} = (\tilde{\rho}_{m,n}^{+,-})^*$]

$$\begin{aligned}\frac{d\tilde{\rho}_{N,M}^{+,+}}{dt} &= \frac{\gamma_\phi}{2}\Big[(\cos2\theta_M\cos2\theta_N - 1)\,\tilde{\rho}_{N,M}^{+,+} \\ &\quad -e^{-it\beta_M}\sin2\theta_M\cos2\theta_N\tilde{\rho}_{N,M}^{+,-} \\ &\quad -e^{it\beta_N}\sin2\theta_N\cos2\theta_M(\tilde{\rho}_{M,N}^{+,-})^* \\ &\quad +e^{it(\beta_N-\beta_M)}\sin2\theta_M\sin2\theta_N\tilde{\rho}_{N,M}^{-,-}\Big] \end{aligned} \quad (9)$$

$$\begin{aligned}\frac{d\tilde{\rho}_{N,M}^{-,-}}{dt} &= \frac{\gamma_\phi}{2}\Big[(\cos2\theta_M\cos2\theta_N - 1)\,\tilde{\rho}_{N,M}^{-,-} \\ &\quad +e^{-it\beta_N}\sin2\theta_N\cos2\theta_M\tilde{\rho}_{N,M}^{+,-} \\ &\quad +e^{it\beta_M}\sin2\theta_M\cos2\theta_N(\tilde{\rho}_{M,N}^{+,-})^* \\ &\quad +e^{-it(\beta_N-\beta_M)}\sin2\theta_M\sin2\theta_N\tilde{\rho}_{N,M}^{+,+}\Big] \end{aligned} \quad (10)$$

$$\begin{aligned}\frac{d\tilde{\rho}_{N,M}^{+,-}}{dt} &= -\frac{\gamma_\phi}{2}\Big[(\cos2\theta_M\cos2\theta_N + 1)\,\tilde{\rho}_{N,M}^{+,-} \\ &\quad +e^{it\beta_M}\sin2\theta_M\cos2\theta_N\tilde{\rho}_{N,M}^{+,+} \\ &\quad -e^{it\beta_N}\sin2\theta_N\cos2\theta_M\tilde{\rho}_{N,M}^{-,-} \\ &\quad -e^{it(\beta_N+\beta_M)}\sin2\theta_M\sin2\theta_N(\tilde{\rho}_{M,N}^{+,-})^*\Big]\,. \end{aligned} \quad (11)$$

When one considers the pair of equations

$$\frac{d}{dt}A(t) = -qe^{itw}B(t)\ ,\ \frac{d}{dt}B(t) = -qe^{-itw}A(t) \quad (12)$$

with constant parameters q and w, the solution is

$$\begin{aligned}A &= \frac{(w_+A_0 - iqB_0)e^{itw_-/2} - (w_-A_0 - iqB_0)e^{itw_+/2}}{r} \quad (13)\\ B &= \frac{(w_+B_0 + iqA_0)e^{-itw_-/2} - (w_-B_0 + iqA_0)e^{-itw_+/2}}{r}\,,\end{aligned}$$

where $r = \sqrt{w^2-4q^2}$ and $w_\pm \equiv (w\pm r)/2$. For $|q/w| \ll 1$ one has $A \simeq A_0$, $B \simeq B_0$, which is equivalent to $dA/dt \simeq 0$, $dB/dt \simeq 0$ in equation (12), provided one neglects the "frequency shifts" of the order $\mathrm{O}(q^2/w)$. This observation constitutes the method of RWA [34, 35], which allows one to neglect the rapidly oscillating terms in differential equations for probability amplitudes. Hence, for $\beta_N \gg \gamma_\phi$ one can neglect the second and the third lines in equations (9) – (11) and the fourth line in equation (11). Moreover, for nondiagonal elements one can also neglect the fourth line in equations (9) – (10). Similar reasoning holds for the atomic and cavity dampings.

Therefore, by choosing resonant modulation frequencies and performing RWA one obtains time-independent coupled differential equations for the matrix elements of $\tilde{\rho}$ that can be solved analytically or numerically. The general solution can be quite cumbersome, so in this work we shall pursue analytically only the asymptotic behavior, obtained by setting the left-hand side of equations (9) – (11) to zero.

III. TWO-EXCITATIONS BEHAVIOR

A. Photon generation from vacuum in resonant regime

First we study the photon creation from the initial zero-excitation state (ZES) $|g,0\rangle$. In the resonant regime, $\Delta_- = 0$, the resonant modulation frequency was found two decades ago [4] and reads

$$\eta^{(r)} = 2\omega_0 + \mathcal{R} g_0 \sqrt{2}\ , \ \mathcal{R} = \pm\,. \tag{14}$$

The effective Hamiltonian is $\tilde{H} = \theta|\varphi_{0,-}\rangle\langle\varphi_{2,\mathcal{R}}| + h.c.$, where

$$\theta = i g_0 \mathcal{R} \frac{\sqrt{2}}{4} \Upsilon^{(r)} \tag{15}$$

$$\Upsilon^{(r)} = \frac{\varepsilon_\omega^{(r)}}{2\omega_0} + \frac{\varepsilon_\Omega^{(r)}}{2\omega_0} - \frac{\varepsilon_g^{(r)}}{g_0} + \mathcal{R} i\sqrt{2}\frac{\varepsilon_\chi^{(r)}}{g_0}\ . \tag{16}$$

Here $\Upsilon^{(r)}$ denotes the dimensionless collective modulation depth [35]. The analytical solution for this Hamiltonian in absence of losses is straightforward [see equations (35)–(37) below] and consists of periodic oscillations between the states $|\varphi_{0,-}\rangle \leftrightarrow |\varphi_{2,\mathcal{R}}\rangle$.

In the presence of dissipation described by SME, under the pure atomic damping we obtain the nonzero asymptotic probabilities of dressed states ($\rho_N^{\mathcal{T}} \equiv \langle\varphi_{N,\mathcal{T}}|\hat{\rho}|\varphi_{N,\mathcal{T}}\rangle$)

$$\rho_0^- = \frac{|\theta|^2 + (\gamma/4)^2}{3\,|\theta|^2 + (\gamma/4)^2}\,,\ \rho_2^{\mathcal{R}} = \frac{|\theta|^2}{3\,|\theta|^2 + (\gamma/4)^2} \tag{17}$$

and $\rho_1^{\pm} = \frac{1}{2}\rho_2^{\mathcal{R}}$. For the pure atomic dephasing we obtain $\rho_0^- = \rho_2^{\pm} = \frac{1}{3}$ and for the pure cavity relaxation

$$\begin{aligned} \rho_0^- &= \frac{|\theta|^2 + (3\kappa/4)^2}{5\,|\theta|^2 + (3\kappa/4)^2}\,,\ \rho_2^{\mathcal{R}} = \frac{|\theta|^2}{5\,|\theta|^2 + (3\kappa/4)^2} \\ \rho_1^{\mathcal{R}} &= \frac{1}{2}(\sqrt{2}+1)^2\rho_2^{\mathcal{R}}\,,\ \rho_1^{-\mathcal{R}} = \frac{1}{2}(\sqrt{2}-1)^2\rho_2^{\mathcal{R}}\,. \end{aligned} \tag{18}$$

Hence dissipation affects dramatically the unitary dynamics, although excitations can still be created whenever $\kappa, \gamma \ll |\theta|$.

For our tentative parameters we obtain $|\theta| \sim 10^{-3} g_0$, so the periodic generation of the state $|\varphi_{2,\mathcal{R}}\rangle$ could be observed without difficulties in current experiments. This is illustrated in figure 1a where we use the parameters $\omega_0/2\pi = 8\,\mathrm{GHz}$, $g_0 = 5\times10^{-2}\omega_0$, $\Delta_- = 0$, $\varepsilon_\Omega = 5\times10^{-2}\Omega_0$, $\eta^{(r)} = 2\omega_0 + g_0\sqrt{2}$ and consider moderate dissipation rates $\kappa = \gamma = \gamma_\phi = 2\times10^{-4} g_0$. We plot the average photon number $\langle\hat{n}\rangle$, the Mandel factor $Q = [\langle(\Delta\hat{n})^2\rangle - \langle\hat{n}\rangle]/\langle\hat{n}\rangle$ (that quantifies the spread of the photon number distribution) and the atomic excitation probability P_e. We see that both models of dissipation predict identical results and several oscillations of $\langle\hat{n}\rangle$, Q and P_e with high visibility could be observed within the time interval of 500 ns.

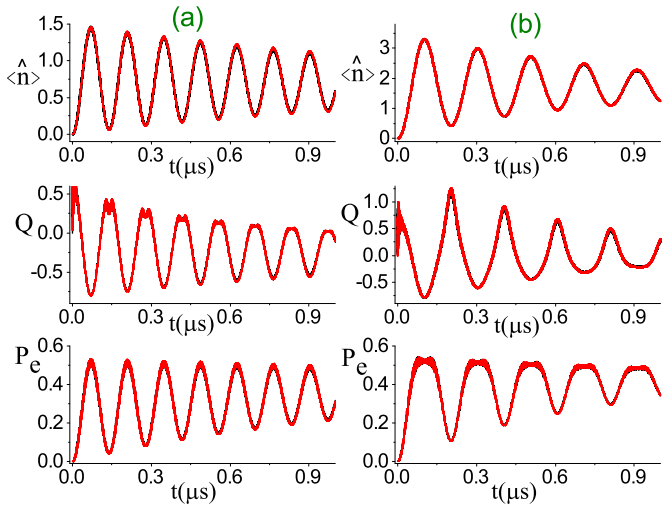


FIG. 1: Photon generation from ZES in the resonant regime. **(a)** One-tone modulation (section III A). **(b)** Two-tone modulation (section IV A). Black (red) lines stand for SME (DPME).

B. Anti-Jaynes-Cummings (AJC) regime

Now we consider the photon generation from ZES in the dispersive regime, $|\Delta_-|/2 \gg g_0\sqrt{n_{\max}}$, where $n_{\max}$ is the maximum number of excitations. The resonant modulation frequency is

$$\eta^{(J)} = \Delta_+ - 2\,(\delta_- - \delta_+) \tag{19}$$

where δ_- (δ_+) is the standard dispersive (Bloch-Siegert) shift given by $\delta_\pm = g_0^2/\Delta_\pm$ and $\Delta_+ \equiv (\omega_0 + \Omega_0)$ (we neglected higher order corrections to $\eta^{(J)}$ [35]). The unitary dynamics is described by the Anti-Jaynes-Cummings (AJC) Hamiltonian [6, 20, 21], which in the dressed picture reads $\tilde{H} = \theta|\varphi_{0,\mathcal{D}}\rangle\langle\varphi_{2,-\mathcal{D}}| + h.c.$,

$$\theta = i\frac{1}{2} g_0 \mathcal{D} \Upsilon^{(J)} \tag{20}$$

$$\Upsilon^{(J)} = -\frac{\varepsilon_\omega^{(J)}}{\Delta_+} - \frac{\varepsilon_\Omega^{(J)}}{\Delta_+} + \frac{\varepsilon_g^{(J)}}{g_0} + i\frac{2\varepsilon_\chi^{(J)}}{\Delta_-}\ . \tag{21}$$

Here $\mathcal{D} \equiv \Delta_-/|\Delta_-| = \pm$ is the "detuning symbol" and we denote $|\varphi_{0,\mathcal{D}}\rangle \equiv |\varphi_{0,-}\rangle$.

For SME we find that under pure atomic dephasing the asymptotic solution is $\rho_0^- = \rho_2^{\pm} = \frac{1}{3}$, with all other probabilities equal to zero. In the presence of pure atomic and cavity dampings we get the asymptotic nonzero probabilities (to the second order in g_0/Δ_-)

$$\rho_2^{-\mathcal{D}} = \frac{\kappa\left(1 - \frac{g_0^2}{\Delta_-^2}\right) + \gamma\frac{g_0^2}{\Delta_-^2}}{\kappa\frac{g_0^2}{\Delta_-^2} + \gamma\left(1 - 3\frac{g_0^2}{\Delta_-^2}\right)}\rho_1^{\mathcal{D}} \tag{22}$$

$$\rho_1^{-\mathcal{D}} = \frac{\kappa\left(1+\frac{g_0^2}{\Delta_-^2}\right)+\gamma\frac{g_0^2}{\Delta_-^2}}{\kappa\frac{g_0^2}{\Delta_-^2}+\gamma\left(1-\frac{g_0^2}{\Delta_-^2}\right)}\rho_2^{-\mathcal{D}} \tag{23}$$

$$\rho_0^- = \left[1+\left(\frac{\kappa+\gamma+2\frac{g_0^2}{\Delta_-^2}(\kappa-\gamma)}{2|\theta|}\right)^2\right]\rho_2^{-\mathcal{D}}, \tag{24}$$

where ρ_0^- can be easily found from the normalization condition. Once again the dissipation changes drastically the dynamics, but for $\kappa,\gamma \ll |\theta|$ excitations are still generated. In particular, for pure atomic (cavity) damping and $\gamma \ll |\theta|$ ($\kappa \ll |\theta|$) we obtain asymptotically $\rho_1^{\mathcal{D}} \approx 1$ ($\rho_1^{-\mathcal{D}} \approx 1$), so only one photon (one atomic excitation) is generated.

For our tentative parameters we obtain $|\theta| \sim 10^{-3}g_0$, of the same order of magnitude as in section III A, so this effect could also be implemented in circuit QED with current technology. This is illustrated in figure 2a for parameters $\omega_0/2\pi = 8\,\mathrm{GHz}$, $g_0 = 5\times10^{-2}\omega_0$, $\Delta_- = 8g_0$, $\varepsilon_\Omega = 5\times10^{-2}\Omega_0$, $\eta^{(J)} = \lambda_{2,-} - \lambda_0 + 2\delta_+ \times 0.954$ and $\kappa = \gamma = \gamma_\phi = g_0\times10^{-4}$. Once again the results are almost indistinguishable for the two dissipation models and the periodic generation of one cavity and one atomic excitations is easily observable on timescales of the order of 500 ns. We notice that two excitations can also we generated from nonvacuum initial states for $\eta^{(J)} = \Delta_+ - 2k(\delta_- - \delta_+)$, where k is an integer and the corresponding generation rate in equation (20) becomes $\theta\sqrt{k}$ [21, 35].

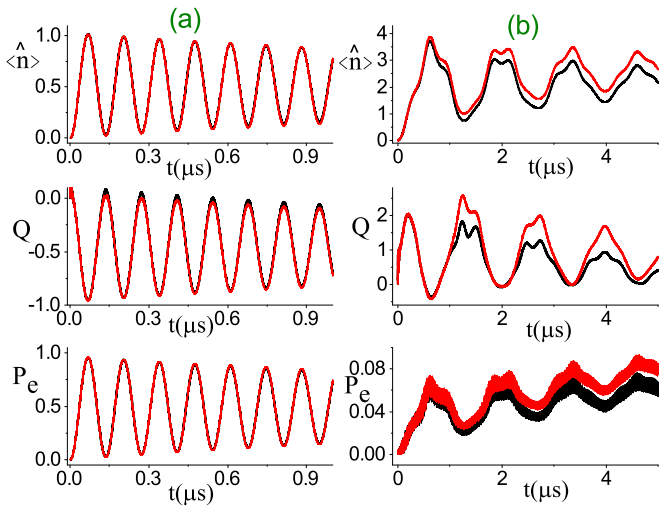


FIG. 2: Photon generation from ZES in the dispersive regime. **(a)** AJC behavior (section III B). **(b)** DCE behavior (section V). Black (red) lines stand for SME (DPME).

C. Anti-DCE regime

The Anti-DCE behavior was predicted recently in [35]. It occurs in the dispersive regime and consists of coherent annihilation of two system excitations via the coupling $|\varphi_{k,\mathcal{D}}\rangle \leftrightarrow |\varphi_{k-2,-\mathcal{D}}\rangle$ for a given value of $k \geq 3$, roughly equivalent to the transition $|g,k\rangle \leftrightarrow |e,k-3\rangle$. For the initial state $|g\rangle\langle g| \otimes \hat{\rho}_{\mathrm{field}}$ three photons are subtracted from the field due to the time-modulation of the system parameters, so the denomination Anti-DCE seems appropriate. Anti-DCE is implemented for the modulation frequency

$$\eta_k^{(A)} = 3\omega_0 - \Omega_0 + 2(\delta_- - \delta_+)(k-1)\,, \tag{25}$$

where $k \geq 3$ and the dressed-picture Hamiltonian is $\tilde{H} = \theta^*|\varphi_{k,\mathcal{D}}\rangle\langle\varphi_{k-2,-\mathcal{D}}| + h.c.$,

$$\theta = i\mathcal{D}\frac{\delta_-\Omega_0 g_0}{2\omega_0\Delta_-}\sqrt{k(k-1)(k-2)}\Upsilon^{(A)} \tag{26}$$

$$\Upsilon^{(A)} = \frac{\varepsilon_\omega^{(A)}}{2\omega_0+\Delta_-} + \frac{\omega_0+\Delta_-}{2\omega_0+\Delta_-}\frac{\varepsilon_\Omega^{(A)}}{\Omega_0} - \frac{\varepsilon_g^{(A)}}{g_0}\,. \tag{27}$$

This phenomenon occurs only for the modulation of ω, Ω or g, so it cannot be implemented by the parametric down-conversion process in which only $\varepsilon_\chi \neq 0$. For our tentative parameters, $|\Delta_-| \sim 10g_0$ and $k \sim 5$, we get $|\theta| \sim 10^{-4}g_0$, so Anti-DCE is a rather weak effect that requires fine-tuning of the modulation frequency and a prolonged maintenance of perturbation. Still, the transition rate $|\theta|$ is slightly greater than the state-of-the-art dissipation rates, so this effect lies on the threshold of implementability with current technology.

For SME, under pure atomic dephasing we obtain asymptotically $\rho_k^{\pm} = \rho_{k-2}^{\pm}$ and $\rho_l^+ = \rho_l^-$ for $l > 0$, so for large times the dephasing changes completely the expected behavior. Anti-DCE behavior is also strongly affected by the cavity relaxation, when one gets approximately

$$\begin{aligned}\frac{d\tilde{\rho}_N^{\mathcal{D}}}{d(\kappa t)} &= (N+1)\left(1-\frac{g_0^2}{\Delta_-^2}\right)\tilde{\rho}_{N+1}^{\mathcal{D}} \\ &+\frac{g_0^2}{\Delta_-^2}\tilde{\rho}_{N+1}^{-\mathcal{D}} - N\left(1-\frac{g_0^2}{\Delta_-^2}\right)\tilde{\rho}_N^{\mathcal{D}}\end{aligned} \tag{28}$$

$$\begin{aligned}\frac{d\tilde{\rho}_{N,N}^{-\mathcal{D}}}{d(\kappa t)} &= N\left(1+\frac{g_0^2}{\Delta_-^2}\right)\tilde{\rho}_{N+1}^{-\mathcal{D}} \\ &-\left(N-1+\frac{g_0^2}{\Delta_-^2}N\right)\tilde{\rho}_N^{-\mathcal{D}}.\end{aligned} \tag{29}$$

Similar formulae hold for the pure atomic damping:

$$\begin{aligned}\frac{d\tilde{\rho}_N^{\mathcal{D}}}{d(\gamma t)} &= \left(1-\frac{g_0^2}{\Delta_-^2}(2N+1)\right)\tilde{\rho}_{N+1}^{-\mathcal{D}} \\ &+\frac{g_0^2}{\Delta_-^2}(N+1)\tilde{\rho}_{N+1}^{\mathcal{D}} - \frac{g_0^2}{\Delta_-^2}N\tilde{\rho}_N^{\mathcal{D}}\end{aligned} \tag{30}$$

$$\frac{d\tilde{\rho}_N^{-\mathcal{D}}}{d(\gamma t)} = \frac{g_0^2}{\Delta_-^2} N \tilde{\rho}_{N+1}^{-\mathcal{D}} - \left(1 - \frac{g_0^2}{\Delta_-^2} N\right) \tilde{\rho}_N^{-\mathcal{D}}. \qquad (31)$$

In both cases the system state goes asymptotically to ZES. This did not happen in the phenomena analyzed in sections III A and III B because there the ZES was coupled to 2-excitations states by the modulation, resulting in nonvacuum equilibrium state.

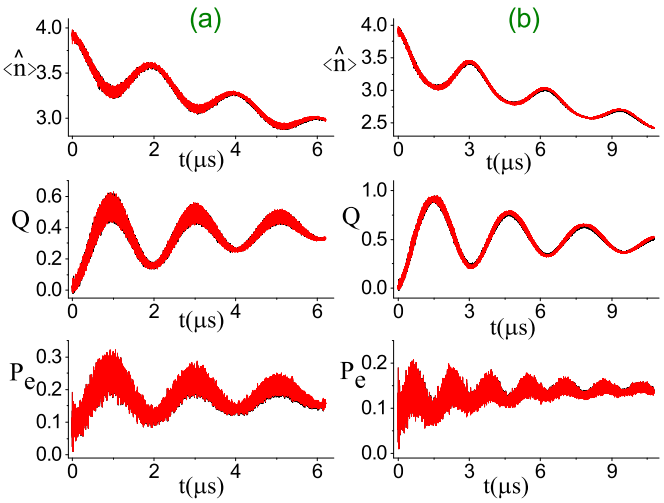


FIG. 3: Coherent photon annihilation in the dispersive regime for initial coherent state $|g\rangle \otimes |\alpha\rangle$. **(a)** Anti-DCE behavior (section III C). **(b)** Enhanced Anti-DCE behavior (section IV B). Black (red) lines stand for SME (DPME).

Figure 3a assesses the feasibility of experimental observation of Anti-DCE for the initial coherent state $|g\rangle \otimes |\alpha\rangle$. We use the values $\alpha = 2$, $\omega_0/2\pi = 8\,\mathrm{GHz}$, $g_0 = 5\times10^{-2}\omega_0$, $\Delta_- = 8g_0$, $\varepsilon_\Omega = 5\times10^{-2}\Omega_0$, $\kappa = 10^{-5}g_0$, $\gamma = \gamma_\phi = 5\times10^{-5}g_0$ and $\eta_4^{(A)} = \lambda_{4,+} - \lambda_{2,-} - 2\delta_+ \times 2.791$. Both master equations predict practically identical results and for initial times the system exhibits the expected behavior, characterized by the periodic reduction of the average photon number accompanied by the partial excitation of the atom and modification of the field statistics from Poissonian to super-Poissonian. The curves corresponding to $\langle\hat{n}\rangle$, Q and P_e exhibit broad widths due to fast oscillations associated with off-resonant exchange of excitations between the atom and the field that occurs on timescales ($\sim |\Delta_-|^{-1}$) much smaller that the characteristic time of Anti-DCE. For larger times the system tends to the ZES and the amplitude of oscillations, as well as the associated visibility, decrease. Yet the main features of Anti-DCE could be resolved in experiments with the current state-of-the-art parameters on timescales of a few μs.

IV. FOUR-EXCITATIONS BEHAVIOR

A. Enhanced photon generation from vacuum in resonant regime

Now we consider the two-tone multi-modulation applied simultaneously to Ω and g, with one frequency given by equation (14) and the second

$$\eta^{(r2)} = 2\omega_0 + g_0\sqrt{2}(\sqrt{2}\mathcal{R}_2 - \mathcal{R}) \ , \ \mathcal{R}, \mathcal{R}_2 = \pm \ . \qquad (32)$$

For initial ZES the effective Hamiltonian reads $\tilde{H} = \theta|\varphi_{0,-}\rangle\langle\varphi_{2,\mathcal{R}}| + \theta_2|\varphi_{2,\mathcal{R}}\rangle\langle\varphi_{4,\mathcal{R}_2}| + h.c.$, where θ is given by (15) and

$$\theta_2 = ig_0\mathcal{R}_2\frac{\sqrt{3}}{4}\Upsilon^{(r2)} \qquad (33)$$

$$\Upsilon^{(r2)} = \frac{\varepsilon_\omega^{(r2)}}{2\omega_0} + \frac{\varepsilon_\Omega^{(r2)}}{2\omega_0} - \frac{\varepsilon_g^{(r2)}}{g_0} + i\mathcal{R}_2\frac{\varepsilon_\chi^{(r2)}}{g_0}(2 + \mathcal{R}\mathcal{R}_2\sqrt{2}) \ . \qquad (34)$$

It is worth writing first the solution for the unitary evolution. We expand the interaction-picture wavefunction as $|\tilde{\psi}\rangle = A|\varphi_{0,-}\rangle + B|\varphi_{2,\mathcal{R}}\rangle + C|\varphi_{4,\mathcal{R}_2}\rangle + \sum(\cdots)$, where $\sum(\cdots)$ denotes the other terms not coupled by the Hamiltonian and we assume real probability amplitudes. For the initial condition $B_0 = 0$ we find

$$A = \left(A_0 + \frac{\theta_2}{\theta^*}C_0\right)\cos Rt + \frac{\theta_2}{R^2\theta^*}\left[2\theta^*\theta_2^* A_0 - 2\theta_2^*(\theta^* A_0 + \theta_2 C_0)\cos^2\frac{1}{2}Rt - (|\theta|^2 - |\theta_2|^2)C_0\right] \qquad (35)$$

$$B = -i\frac{(\theta^* A_0 + \theta_2 C_0)\sin Rt}{R} \qquad (36)$$

$$C = \frac{2\theta_2^*(\theta^* A_0 + \theta_2 C_0)\cos^2\frac{1}{2}Rt}{R^2} + \frac{(|\theta|^2 - |\theta_2|^2)C_0 - 2\theta^*\theta_2^* A_0}{R^2}, \qquad (37)$$

where $R \equiv \sqrt{|\theta|^2 + |\theta_2|^2}$. One can transfer the populations entirely from $\{A,C\}$ to C at the smallest time $Rt_{\min} = \pi$ by choosing $\theta_2 = x\theta^*$, $x = \left(C_0 \pm \sqrt{C_0^2 + A_0^2}\right)/A_0$. In the present case $x = \pm1$, so one can create the pure dressed state $|\varphi_{4,\mathcal{R}_2}\rangle$ at the time $t_{\min} = \pi/(|\theta|\sqrt{2})$.

For the pure atomic dephasing described by SME we get in the asymptotic limit $\rho_0^- = \rho_2^\pm = \rho_4^\pm = 1/5$, while for the pure atomic damping the nonzero probabilities are

$$\rho_0^- = \left(\frac{2|\theta|^2 + (\gamma/4)^2}{|\theta|^2} - 2\frac{|\theta|^2 - (\gamma/4)^2}{3|\theta|^2 + \gamma^2/4}\right)\rho_2^{\mathcal{R}} \qquad (38)$$

$$\rho_4^{\mathcal{R}_2} = \frac{4\left|\theta\right|^2}{3\left|\theta\right|^2+\gamma^2/4}\rho_2^{\mathcal{R}} \tag{39}$$

$$\rho_1^{\pm} = \frac{1}{2}\frac{5\left|\theta\right|^2+\gamma^2/4}{3\left|\theta\right|^2+\gamma^2/4}\rho_2^{\mathcal{R}} \tag{40}$$

$$\rho_3^{\pm} = \rho_2^{-\mathcal{R}} = \frac{1}{2}\rho_4^{\mathcal{R}_2}\ , \tag{41}$$

where ρ_0^- can be found from the normalization condition. Similar expressions are obtained for the pure cavity damping, so we conclude that for $\kappa,\gamma \ll |\theta|$ four excitations can be generated from vacuum. For our tentative parameters we get $|\theta|, |\theta_2| \sim 10^{-3} g_0$, so this effect can also be implemented with current technology.

We illustrate the typical outcome in figure 1b, where we consider the modulation of Ω with frequency $\eta^{(r)} = 2\omega_0 + g_0\sqrt{2}$ and modulation of g with frequency $\eta^{(r2)} = 2\omega_0 + g_0(2-\sqrt{2})$. Other parameters are $\omega_0/2\pi = 8\,\mathrm{GHz}$, $g_0 = 5\times 10^{-2}\omega_0$, $\Delta_- = 0$, $\varepsilon_\Omega = 5\times 10^{-2}\Omega_0$, $\varepsilon_g = 1.97\times 10^{-2} g_0$, $w_\Omega^{(r)} = w_g^{(r2)} = 1$ and $\kappa = \gamma = \gamma_\phi = 2\times 10^{-4} g_0$. We see that even for moderate values of dissipation rates the enhanced photon generation due to multi-modulation can still be observed. Moreover, the predictions of SME and DPME are almost indistinguishable.

B. Photon annihilation in enhanced Anti-DCE regime

One can enhance the Anti-DCE behavior by combining the modulation frequency (25) with the second frequency

$$\eta_k^{(A2)} = \Delta_+ - 2\left(\delta_- - \delta_+\right)(k-3)\ , \tag{42}$$

where $k \geq 4$ is an integer. The effective Hamiltonian becomes $\tilde{H} = \theta^* |\varphi_{k,\mathcal{D}}\rangle\langle\varphi_{k-2,-\mathcal{D}}| + \theta_2^* |\varphi_{k-2,-\mathcal{D}}\rangle\langle\varphi_{k-4,\mathcal{D}}| + h.c.$, where θ is given by (26) and

$$\theta_2 = i\frac{1}{2} g_0 \mathcal{D}\sqrt{k-3}\,\Upsilon^{(A2)} \tag{43}$$

$$\Upsilon^{(A2)} = -\frac{\varepsilon_\omega^{(A2)}}{\Delta_+} - \frac{\varepsilon_\Omega^{(A2)}}{\Delta_+} + \frac{\varepsilon_g^{(A2)}}{g_0} + i\frac{2\varepsilon_\chi^{(A2)}}{\Delta_-}\,. \tag{44}$$

In this regime one combines simultaneously the coupling $|\varphi_{k,\mathcal{D}}\rangle \longrightarrow |\varphi_{k-2,-\mathcal{D}}\rangle$ via Anti-DCE with the coupling $|\varphi_{k-2,-\mathcal{D}}\rangle \rightarrow |\varphi_{k-4,\mathcal{D}}\rangle$ via the AJC behavior, obtaining the annihilation of four excitations. In the dispersive regime this corresponds to subtraction of four photons from the state $|g,k\rangle\langle g,k|$. The effective Hamiltonian is similar to the one considered in section IV A, so the formulae (35) – (37) can be applied after appropriate substitutions. If the initial cavity state is known and the population of the excited atomic state is negligible, one can transfer completely the populations of $\{|\varphi_{k,\mathcal{D}}\rangle, |\varphi_{k-4,\mathcal{D}}\rangle\}$ to $|\varphi_{k-4,\mathcal{D}}\rangle$ at specific times without affecting the other states, so four photons are indeed annihilated. If the initial statistics is not known, the transfer is not complete because the required value of θ_2 cannot be determined beforehand.

For SME we reach the same conclusions about the asymptotic behavior as in section III C, supplemented by the additional condition $\rho_k^{\mathcal{D}} = \rho_{k-2}^{\mathcal{D}} = \rho_{k-4}^{\mathcal{D}}$ under pure atomic dephasing. As the associated transition rates are similar to the one estimated in section III C, the enhanced Anti-DCE also lies at the threshold of experimental feasibility, provided two simultaneous fine-tuned modulations can be sustained for a time interval of a few μs. This is illustrated in figure 3b for the initial coherent state $|g\rangle \otimes |\alpha\rangle$ and the simultaneous modulation of Ω and g. We used the parameters of figure 3a, $\varepsilon_g = 9.91\times 10^{-4} g_0$, $\eta_4^{(A2)} = \lambda_{2,-} - \lambda_0 + 2\delta_+ \times 0.954$ and nonzero modulation weights $w_\Omega^{(A)} = w_g^{(A2)} = 1$. We see that the reduction of $\langle\hat{n}\rangle$ is stronger than in the standard Anti-DCE case, occurring at larger timescales; the $Q-$factor increases while the atomic excitation probability undergoes faster oscillations and is slightly smaller than in figure 3a because the transfer of population from $|g,4\rangle$ to $|e,1\rangle$ is only partial. Moreover, SME and DPME predict almost identical behaviors, with minor quantitative differences appearing only for larger times $t \gtrsim 5\,\mu$s.

V. DYNAMICAL CASIMIR EFFECT (DCE) WITH SINGLE QUBIT

In the dispersive regime one can create many pairs of excitations from the initial ZES for the modulation frequency

$$\eta^{(d)} = 2(\omega_0 + \delta_- - \delta_+)\,. \tag{45}$$

The dynamics is described by the effective Hamiltonian

$$\tilde{H} = \sum_{m=0}^{\infty} \theta_m e^{-it(\lambda_{m+2,\mathcal{D}} - \lambda_{m,\mathcal{D}} - \eta^{(d)})} |\varphi_{m,\mathcal{D}}\rangle\langle\varphi_{m+2,\mathcal{D}}| + h.c., \tag{46}$$

$$\theta_m = i\frac{\delta_-\Omega_0}{2\Delta_+}\sqrt{(m+1)(m+2)}\,\Upsilon^{(d)} \tag{47}$$

$$\Upsilon^{(d)} = \frac{\varepsilon_\omega^{(d)}}{\omega_0} + \frac{\varepsilon_\Omega^{(d)}}{\Omega_0} - 2\frac{\varepsilon_g^{(d)}}{g_0} + i\frac{\Delta_+}{\Omega_0}\frac{\varepsilon_\chi^{(d)}}{\delta_-}\,, \tag{48}$$

so only the states $|\varphi_{2m,\mathcal{D}}\rangle \simeq |g,2m\rangle$ are populated during the dissipationless evolution. The unitary dynamics of the Hamiltonian was studied in [35], where it was shown that the photon generation from vacuum suffers saturation due to effective Kerr nonlinearity (of magnitude g_0^4/Δ_-^3), and $\langle\hat{n}\rangle$ exhibits a collapse–revival behavior as function of time. Simple analytical expressions cannot be obtained for this case because many dressed states

are coupled simultaneously and the argument of the exponentials depends on the index m in nontrivial manner.

For SME the pure atomic damping is equivalent to the pure cavity damping with effective relaxation rate $\kappa_{ef} = \gamma(g_0/\Delta_-)^2$ (for the initial ZES and under RWA). The asymptotic solution for a similar problem (parametric amplification in the presence of Kerr nonlinearity and cavity relaxation) was obtained two decades ago using the method of potential solutions for the corresponding Fokker-Planck equation [45, 46]. However, the asymptotic solution is of little use in our case because the photon statistics during the transient time can be quite different from the asymptotic one [35], so we rely entirely on numerical simulations.

For our tentative parameters we estimate $|\theta_0^{(d)}| \sim 10^{-4} g_0$, so in principle the single-qubit DCE could be observed in the current state-of-the-art architectures. This is confirmed in figure 2b where we show the expected behavior for parameters $\omega_0/2\pi = 8\,\mathrm{GHz}$, $g_0 = 5\times10^{-2}\omega_0$, $\Delta_- = 8g_0$, $\varepsilon_\Omega = 5\times10^{-2}\Omega_0$, $\kappa = \gamma = \gamma_\phi = 5\times10^{-5} g_0$ and $\eta^{(d)} = \lambda_{2,+} - \lambda_0 - 2\delta_+ \times 1.02$. Both dissipation models predict identical results for initial times; for times $t \gtrsim 1\,\mu$s some small quantitative differences appear without changing the overall behavior. The saturation in photon growth occurs due to the nonzero values of $(\lambda_{m+2,\mathcal{D}} - \lambda_{m,\mathcal{D}} - \eta^{(d)}) \propto m$ in (46) for large values of m, and is not related to the presence dissipation. We see that photons can be generated and the collapse–revival of $\langle\hat{n}\rangle$ can be observed on the timescale of a few μs. Notice that the collapse–revival behavior is not associated to the absorption and reemission of photons by the atom [47, 48], as the atomic excitation probability stays $\lesssim 8\%$ for all times. More photons can be generated if one adds a second modulation frequency or increases $|\Upsilon^{(d)}|$ or Δ_- [35], but in the latter case the parameter $|\theta_m|$ decreases so the process becomes slower and demands more precise tuning of the modulation frequency.

VI. CONCLUSIONS

We estimated the rates of photon creation and annihilation for some nonstationary phenomena induced by fast modulation of qubit parameters in dissipative circuit QED. Two different Markovian master equations ("standard" and "dressed-picture" master equations) were used to account for the common sources of dissipation, and we verified that for the relevant regime of parameters the predicted behaviors are almost identical.

Our results indicate that all the analyzed phenomena could be implemented experimentally with the present technology, provided one can implement modulations with relative depths $|\Upsilon| \sim 10^{-2}$ and frequencies $\eta \sim 15\,\mathrm{GHz}$. The most accessible phenomena ("fast phenomena") are the two- and four-excitations generation from vacuum in the resonant regime (using single- and two-tone modulations, respectively) and the two-excitation generation via the AJC behavior in the dispersive regime. For these effects the photon generation rates are $|\theta| \sim 10^{-3} g_0$, so they could be implemented even in systems with moderate dissipation. On the other hand, generation of several photons from vacuum via DCE and annihilation of two or four excitations via Anti-DCE in the dispersive regime ("slow phenomena") occur at lower rates $|\theta| \sim 10^{-4} g_0$, so only state-of-the-art architectures would allow for their experimental verification. Additionally, the modulation frequency must be fine-tuned with accuracy of the order of $|\theta|$ and maintained for the time interval $\sim 500\,\mathrm{ns}$ for the fast phenomena and $\sim 5\,\mu$s for the slow ones. Although all these requirements are challenging, the verification of the nonstationary phenomena in circuit QED could lead to new manners of generating entangled states by means of the counter-rotating terms in the light–matter interaction Hamiltonian.

Acknowledgments

DSV acknowledges financial support by CAPES (Brazilian agency). AVD acknowledges partial support by CNPq, Conselho Nacional de Desenvolvimento Científico e Tecnológico – Brazil.

[1] Schoelkopf R J and Girvin S M 2008 *Nature* **451** 664
[2] Clarke J and Wilhelm F K 2008 *Nature* **452** 1031
[3] Nation P D *et al.* 2012 *Rev. Mod. Phys.* **84** 1
[4] Dodonov V V 1995 *Phys. Lett.* A **207** 126
[5] Narozhny N B, Fedotov A M and Lozovik Yu E 2001 *Phys. Rev.* A **64** 053807
[6] Dodonov A V *et al.* 2011 *J. Phys.* B **44** 225502
[7] Dodonov A V and Dodonov V V 2012 *Phys. Rev.* A **85** 015805
[8] Fujii T *et al.* 2011 *Phys. Rev.* B **84** 174521
[9] Dodonov A V and Dodonov V V 2011 *Phys. Lett.* A **375** 4261
[10] Dodonov A V and Dodonov V V 2012 *Phys. Rev.* A **86**, 015801
[11] Dodonov A V and Dodonov V V 2013 *Phys. Scr.* T **153** 014017
[12] de Castro A S M, Cacheffo A and Dodonov V V 2013 *Phys. Rev.* A **87** 033809
[13] De Liberato S, Ciuti C and Carusotto I 2007 *Phys. Rev. Lett.* **98** 103602
[14] De Liberato S *et al.* 2009 *Phys. Rev.* A **80** 053810
[15] Benenti G, Siccardi D and Strini G 2014 *Eur. Phys. J.* D **68** 139
[16] Benenti G *et al.* 2014 *Phys. Rev.* A **90** 052313

[17] Felicetti S *et al.* 2015 arXiv:1503.06653
[18] Saito K *et al.* 2006 *Europhys. Lett.* **76** 22
[19] Wubs M, Kohler S and Hanggi P 2007 *Physica E - Low-Dim. Syst. Nanostr.* **40** 187
[20] Dodonov A V *et al.* 2008 arXiv: 0806.4035
[21] Dodonov A V 2009 *J. Phys.: Conf. Ser.* **161** 012029
[22] Werlang T *et al.* 2008 *Phys. Rev.* A **78** 053805
[23] Vacanti G *et al.* 2012 *Phys. Rev. Lett.* **108** 093603
[24] Dodonov A V and Dodonov V V 2012 *Phys. Rev.* A **85** 063804
[25] Carusotto I *et al.* 2012 *Phys. Rev.* A **85** 023805
[26] Dodonov A V and Dodonov V V 2012 *Phys. Rev.* A **85** 055805
[27] Dodonov A V 2013 *Phys. Scr.* **87** 038103
[28] Felicetti S *et al.* 2014 *Phys. Rev. Lett.* **113** 093602
[29] Blais A *et al.* 2004 *Phys. Rev.* A **69** 062320
[30] Wallraff A *et al.* 2004 *Nature* **431** 162
[31] Wilson C M *et al.* 2011 *Nature* **479** 376
[32] Lähteenmäki P *et al.* 2013 *Proc. Nat. Acad. Sci.* **110** 4234
[33] Johansson J R *et al.* 2010 *Phys. Rev.* A **82** 052509
[34] Dodonov A V 2013 *J. Phys.* A **47** 285303
[35] de Sousa I M and Dodonov A V 2015 arXiv:1504.02413
[36] Beaudoin F, Gambetta J M and Blais A 2011 *Phys. Rev.* A **84** 043832
[37] de Castro A S M, Cacheffo A and Dodonov V V 2014 *Phys. Rev.* A **89** 063816
[38] Kirchmair G *et al.* 2013 *Nature* **495** 205
[39] Ristè D *et al.* 2013 *Nature* **502** 350
[40] Sun L *et al.* 2014 *Nature* **511** 444
[41] Vogel W and Welsch D -G 2006 *Quantum Optics* (Berlin: Wiley)
[42] Schleich W P 2001 *Quantum Optics in Phase Space* (Berlin: Wiley)
[43] Rabi I I (1936) Phys Rev **49** 324; Rabi I I (1937) Phys Rev **51** 652
[44] Law C K 1994 *Phys. Rev.* A **49** 433
[45] Kryuchkyan G Yu *et al.* 1995 *Quantum Semiclass. Opt.* **7** 965
[46] Kryuchkyan G Yu and Kheruntsyan K V 1996 *Opt. Commun.* **127** 230
[47] Milburn G J 1990 *Phys. Rev.* A **41** 6567
[48] Milburn G J and Holmes C A 1991 *Phys. Rev.* A **44** 4704